Korean J. Chem. Eng., 35(8), 1636-1641 (2018)
DOI: 10.1007/s11814-018-0056-2

pISSN: 0256-1115
eISSN: 1975-7220

Adsorption of fluoride by the calcium alginate embedded with Mg-Al-Ce trimetal oxides

Aihe Wang*,, Kanggen Zhou*,†, Wei Chen*, Chun Zhang*, Xing Liu*, Quanzhou Chen*, and Fang Liu***

*Institute of Environmental Science and Engineering, School of Metallurgy and Environment, Central South University, Lushan South Road 932, Changsha, 410083, P. R. China
**School of Municipal and Mapping Engineering, Hunan City University, Yingbin East Road 518, Yiyang Hunan, 413000, P. R. China
(*Received 11 July 2017 • accepted 28 March 2018*)

Abstract−Batch experiments were conducted to study the adsorption performance of fluorine removal by the calcium alginate (SA) embedded by the composite Mg-Al-Ce oxides (SA-CMAC). The physical and chemical properties of the SA-CMAC were characterized by XRD, SEM and XPS analysis. The optimum conditions for fluoride removal were determined and the maximum adsorption capacity was 26.12 mg g^{-1}. The co-existing PO_4^{3-} and CO_3^{2-} anions in solution had more effect than the SO_4^{2-} and NO_3^- on the fluoride removal efficiency. The adsorption process of fluorine by SA-CMAC was attributed to ion exchange on the surface of the SA-CMAC. The experimental data fitted both the isotherms and Freundlich well, and the Freundlich model had a little higher correlation coefficient. As the rate determining step, the adsorption process could be best described by the pseudo-second order kinetic model followed by the intra-particle diffusion. The thermodynamic examination demonstrated that the fluoride adsorption on the SA-CMAC beads was reasonably spontaneous and exothermic. The reclaimed adsorbents still could adsorb 65% of the total fluoride in the solution after three cyclic processes using 0.01 mol/L NaOH.

Keywords: Metal Composite Oxides, Calcium Alginate, Fluoride, Adsorption Isotherm, Adsorption Kinetic, Regeneration

INTRODUCTION

Fluorine is one of the essential trace elements for human health, and a small quantity of fluoride can be beneficial to the growth of teeth and bones. However, higher concentration may cause a variety of diseases, such as dental fluorosis, skeletal fluorosis, crippling skeletal fluorosis, osteoporosis, brain damage, neurological disorder and so on [1]. The fluorine in water mainly comes from industrial production. Fluorine-containing industrial wastes are primarily derived from the glass and ceramic industries, semiconductor manufacturing, electroplating, iron work and other production processes [2]. The concentrations of fluorine in different industrial wastewater range from several hundreds to several thousands mol/L. Consequently, fluorine-containing wastewater may bring serious environmental and human health problems if it cannot be effectively treated.

Current methods for treatment mainly include precipitation [3], coagulation [4], electrolysis [5], induced crystallization [6,7], hyperfiltration [8], membrane method [9] and adsorption. Specifically, the adsorption technology was widely adopted for its low costs, ease of treatment and environmental friendliness. The key for the adsorption process is the determination of adsorbents. Presently, the adsorbents for fluoride removal include activated aluminium oxide, bone coal, composite metal oxides and hydrotalcites [10,11]. Composite metal oxides (hydroxide) have been used as the function materials to remove fluoride in wastewater and better results were achieved. The composites containing Fe-Ca-Zr metal oxides were prepared by the co-precipitation method by Dhillon [12], and the maximum adsorbing capacity reached 250 mg/g when the initial pH was 7.0. The adsorbing capacity was 33 mg/g under the optimum conditions when Zn-Cr-LDH [13] adsorbents were employed. The maximum adsorbing capacities of Ce-Fe [14] and La-Zr [15] composites were 60.97 mg/g and 88.5 mg/g, respectively. The hydrous zirconium oxide [16], CeO_2/Al_2O_3 [17], Co-Al [18], Ti-Al [19], Fe-Zr [20] and Mg-Al-Ce [21] composites also presented excellent fluoride affinities. However, such adsorbents are farinose and are difficult to be separated after adsorption owing to small particle sizes, which limit the application of the adsorbents for real projects. To overcome these defects, such function materials can be loaded or embedded on the surface of a carrier, such as calcium alginate, to prepare the granular adsorbents. Currently, the calcium alginate loaded or embedded metal oxides have been successfully applied in the treatment of wastewater containing heavy metals [22] and nitrate [23], but very few studies [24] were found for its application in the treatment of fluorine-containing wastewater.

In this study, the composite Mg-Al-Ce oxides were loaded onto the surface of the calcium alginate to prepare the composite function materials. The adsorption performance of fluorine by the prepared composite function materials was studied. Batch experiments were performed to study the adsorption kinetics and adsorption isotherm. The adsorption mechanism and the effects of pH and the co-existing ions on the adsorption process were presented.

†To whom correspondence should be addressed.
E-mail: zhoukg63@163.com

MATERIALS AND METHODS

1. Materials

All chemicals, including hydrochloric acid, sodium hydroxide, calcium chloride, cerium chloride magnesium chloride, aluminum chloride and sodium alginate, were of analytical grade and used as received. 2.21 g of sodium fluoride was weighted and dissolved in 1 L of distilled water as the stock solution. Solutions with varying fluoride concentrations used in the experiments were prepared by diluting the stock solution.

2. Preparation of Adsorbents

Magnesium chloride, aluminum chloride and cerium chloride were weighed according to the mass ratio of Mg : Al : Ce=20 : 1 : 4. The mixture was then dissolved into 300 mL of distilled water. A certain amount of sodium hydroxide and sodium carbonate was also dissolved into the solution. The prepared solutions were added into a triangular flask with 400 mL of distilled water at 3 mL/min. The pH was determined at 9-10 and the temperature was at 60 °C. When the addition process was over, the miscible liquids stood for 12 h. The mixture was filtered, rinsed with distilled water and dried at 80 °C. The precipitates were collected and roasted at 500 °C in a muffle furnace for five hours. After then, the roasted composite Mg-Al-Ce oxides (CMAC) were obtained.

Sodium alginate and the CMAC were weighed according to the ratio of 1 : 4, and the mixture was dissolved into 100 mL of distilled water; a homogeneous sol solution was obtained by magnetic stirring. 15 g of calcium chloride was dissolved in 500 mL of distilled water to prepare 3% calcium chloride solution. Then, the sol solution was added into the 3% calcium chloride solution to form particles and left standing for 24 h. Afterwards, the precipitates were watered and dried for 24 h in the drying cabinet at 60 °C. The obtained products were recorded as the SA-CMAC.

3. Instrument Analysis

The X-ray diffraction pattern was recorded using X-ray diffractometer (Bruker D8 Discover) with CuKa radiation (40 kv, 40 mA). The SEM-EDS analysis was completed using a scanning electron microscope (FEI Quanta-200). The X-ray photoelectron spectroscopy (XPS) spectra were obtained with an analyzer (ESCALab250Xi) with an Al KR X-ray source (power: 200 W). The spectra were collected at a fixed retarding ratio mode with band-pass energy of 20 eV. The Fourier transform infrared (FT-IR) spectra were obtained on a Nicolet 5700 infrared spectrometer (Nicolet IS10, USA) with a KBr pellet in the range of 4,000-400 cm^{-1}. The concentration of fluoride ions in the solution was determined using fluorine ion selective electrode.

4. Experimental Procedure

4-1. Effect of Initial pH

The initial pH of the solution was regulated at 2, 4, 6, 8, 10, 12 and 13, respectively. The dosage of the SA-CMAC was 5 g and the initial concentration of fluorine was 40 mg/L. The mixture was shaken in the constant temperature bath oscillator for 24 h at the rotating speed of 150 rpm min^{-1}. The concentration of fluorine supernatant was determined after filtration using 0.22 μm filter membrane.

4-2. Adsorption Isotherm

The initial pH of the solution was determined at 6.0. The dosage of the SA-CMAC was 5 g and the initial concentration of fluorine was 10-200 mg L^{-1}. The mixture was shaken in the constant temperature bath oscillator for 24 h at 303 K, 313 K, 308 K and 318 K. The concentration of the fluorine supernatant was determined after filtration using 0.22 μm filter membrane.

4-3. Adsorption Kinetics

The initial pH of the solution was determined at 6.0. The dosage of the SA-CMAC was 5 g and the initial concentration of fluorine was 60 mg L^{-1}. The mixture was shaken in the constant temperature bath oscillator for 24 h at different temperatures of 298 K, 303 K and 308 K. The concentration of fluorine supernatant was determined after filtration using 0.22 μm filter membrane.

4-4. Effect of Co-existing Ion

The initial pH of the solution was determined at 6.0. The dosage of the SA-CMAC was 5 g and the initial concentration of fluorine was 40 mg L^{-1}. The initial co-existing CO_3^{2-}, NO_3^-, PO_4^{3-} and Cl^- were 0.01, 0.03, 0.05, 0.07 and 0.1 mol L^{-1}, respectively. The mixture was shaken in the constant temperature bath oscillator for 24 h at 303 K. The concentration of fluorine supernatant was determined after filtration using 0.22 μm filter membrane.

4-5. Regeneration of the Adsorbents

The initial pH of the solution was also determined at 6.0. The dosage of the SA-CMAC was 5 g and the initial concentration of fluorine was 40 mg/L. The mixture was shaken in the constant tem-

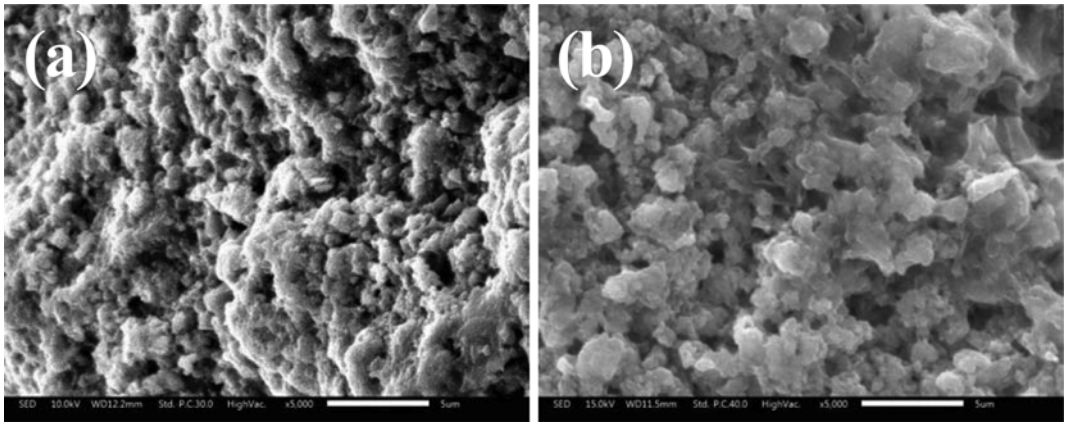

Fig. 1. SEM images of (a) SA-CMAC and (b) SA-CMAC after adsorption.

perature bath oscillator for 24 h at 303 K. When the adsorption process was over, the filtered adsorbents were mixed with NaOH with the concentration of 0.01 mol/L. The concentration of fluorine in the solution after adsorption and desorbed solution was determined. The regeneration of the adsorbents was valued by the triple adsorption-desorption systems.

RESULTS AND DISCUSSION

1. Characterization of the Adsorbents

Fig. 1 presents the SEM analysis of the adsorbents before and after adsorption. The surface of the virgin adsorbent was smooth with large porosity. After adsorption, the porosity of the adsorbent decreased apparently and the surface became rough.

The FT-IR analysis was performed to characterize the adsorbent before and after adsorption and the results are presented in Fig. 2. The stretching vibration absorption peak at 3,427 cm^{-1} was attributed to the O-H bond [25,26]. The peak at 1,627 cm^{-1} was the stretching vibration of the water molecules adsorbed on the surface of the adsorbents, and the peak at 1,627 cm^{-1} resulted from the carbonate ion [27]. The peaks below 500 cm^{-1} were attributed to the vibration of the bond of Me-O (Me: Mg, Al, Ce). According to the FT-TR analysis, the stretching vibration absorption peaks were broadened at different levels, which showed that both -OH and CO_3^{2-} were involved in the adsorption process.

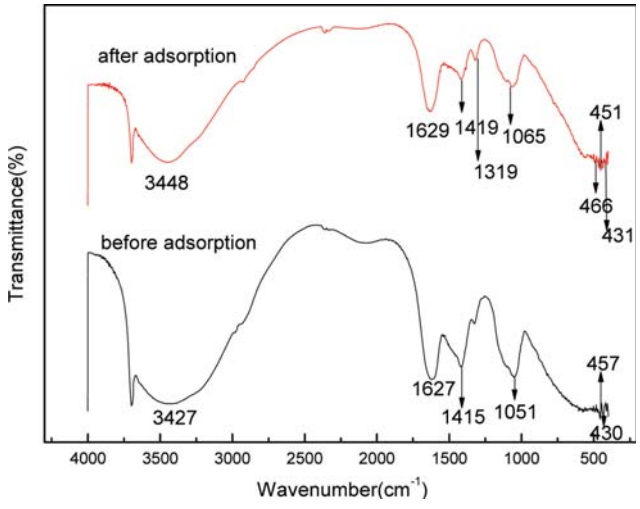

Fig. 2. The FT-IR analysis of SA-CMAC before and after adsorption.

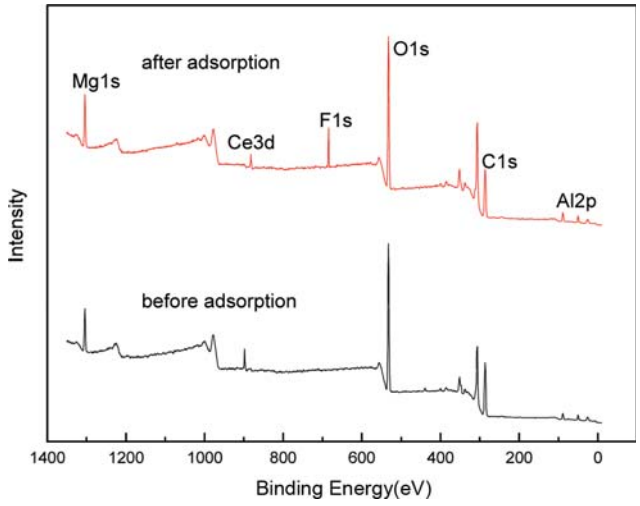

Fig. 3. XPS spectra of SA-CMAC before and after adsorption.

Fig. 3 shows the XPS spectrum analysis of the SA-CMAC after adsorption. The main vibration peaks of the SA-CMAC included the Mg1s, Ce3d, O1s, C1s and Al2p, and the F1s was found at 684.36 eV, confirming that the fluorine was adsorbed by the SA-CMAC. Combined with the FT-IR analysis, the adsorption of fluorine by the SA-CMAC was attributed to the ion exchange on the surface.

2. Effect of pH on the Adsorption of Fluorine by SA-CMAC

The effect of different initial solution pH values on the adsorption of fluorine by SA-CMAC was determined, and the result is presented in Fig. 4. When the initial pH was 2, the adsorbing capacity was 5.21 mg g^{-1} and decreased to 2.21 mg g^{-1} at the pH of 13. When the pH was between 3 and 10, the adsorption capacity was almost unchanged, suggesting that the adsorption of fluorine by the SA-CMAC had a wide range of pH. The competition of the

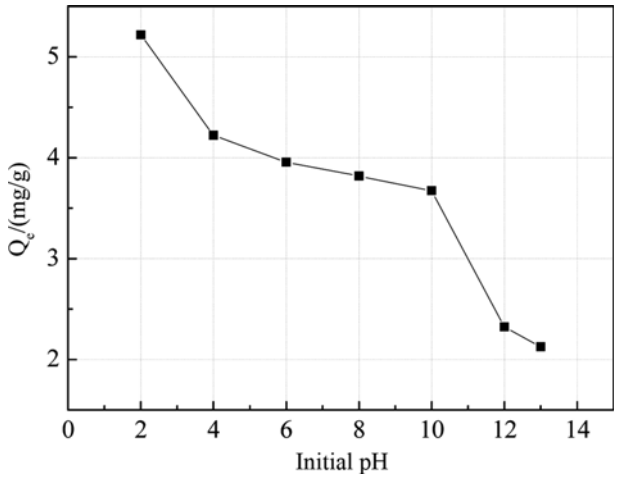

Fig. 4. Effect of pH on the adsorption of fluoride by SA-CMAC.

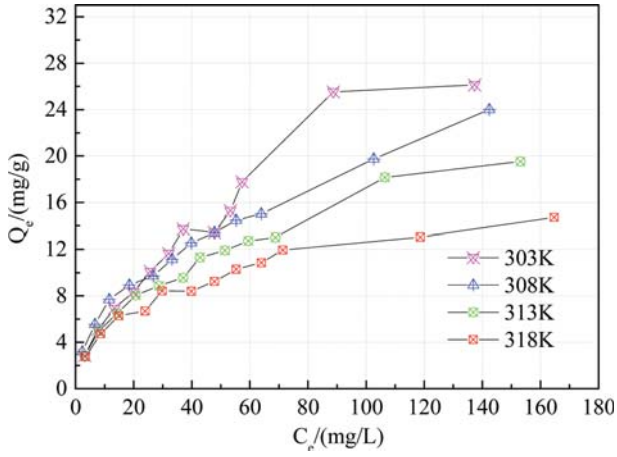

Fig. 5. Adsorption isotherms of fluoride by SA-CMAC.

Table 1. The parameters of adsorption isotherm of fluoride by SA-CMAC

Isotherm equation	Temperature (K)			
	303	308	313	318
Langmuir isotherm				
Q_{max} (mg/g)	36.90	27.40	23.53	16.53
K_L (L/g)	0.0004457	0.0009352	0.0010254	0.0020822
R^2	0.8825	0.9166	0.9422	0.9779
Freundlich isotherm				
K_f (mg/g)	1.344	2.214	1.725	1.838
n	1.586	2.126	2.040	2.369
R^2	0.9891	0.9938	0.9935	0.9810

active sites in most solid-liquid adsorption process was implemented by the hydroxyl. Thus the fluorine was removed by the ion exchanges, and the exchanged hydroxyl and carbonate ions kept the solution with a wide range of pH.

3. Adsorption Isotherm

The adsorption isotherms of fluoride by SA-CMAC at different temperatures are presented in Fig. 5. The Langmuir [28,29] and Freundlich [30,31] adsorption isothermal equations were adopted to analyze the experimental data and the formulas were as follows. The relative analysis results are presented in Table 1.

$$\frac{C_e}{Q_e}=\frac{1}{K_L Q_{max}}+\frac{1}{Q_{max}}C_e \tag{1}$$

$$\lg Q_e=\lg K_F+\frac{\lg C_e}{n} \tag{2}$$

where K_L (L mg^{-1}) and Q_{max} (mg g^{-1}) are the adsorption isotherm constant of Langmuir and the maximum adsorption capacity, respectively, and k_F and n are the adsorption isotherm constants of Freundlich, which are associated with the adsorption strength.

According to the adsorption equilibrium data presented in Table 1, the correlation coefficients from the Freundlich isotherm were higher than those from the Langmuir isotherm, suggesting that the adsorption data fitted the Freundlich isotherm better, and the adsorption on the SA-CMAC was multi-molecular layer adsorption. This indicated that the embedding of CMAC into the polymer SA resulted an inhomogeneous surface. The inhomogeneous distribution led to the inhomogeneous distribution of the active sites. All these results fitted well with the assumptions of the theory of the Freundlich adsorption isotherm. Besides, the value of n was higher than 1, indicating that the adsorption of fluoride by SA-CMAC was preferential.

The thermodynamic adsorption parameters of fluoride adsorbed by SA-CMAC, such as the Gibbs free energy ΔG^0 (kJ mol^{-1}), the entropy change ΔH^0 (kJ mol^{-1}) and the enthalpy change ΔS^0 (J $k^{-1}mol^{-1}$), were determined according to formulas (3), (4) and (5) [32] and the results are presented in Table 2.

$$K_D=\frac{q_e}{C_e} \tag{3}$$

$$\Delta G=-RT\ln K_D \tag{4}$$

Table 2. The thermodynamic adsorption parameters of fluoride by SA-CMAC

Temperature (K)	ΔG^0 (kJ mol^{-1})	ΔH^0 (kJ mol^{-1})	ΔS^0 (J $k^{-1}mol^{-1}$)
303	−1.322	−40.94	−90.93
308	−1.313		
313	−1.262		
318	−1.187		

$$\ln K_D=\frac{\Delta S}{R}-\frac{\Delta H}{RT} \tag{5}$$

The obtained Gibbs free energies (ΔG^0) of the adsorption reaction between 303-318 K were negative values, suggesting that the adsorption of fluoride by SA-CMAC was a spontaneous process. The negative ΔH^0 showed that the reactions were exothermic. The elevated temperature was not conducive to the adsorption reaction and the negative ΔS^0 was an entropy decrease process.

4. Adsorption Kinetics

The adsorption rate of the adsorbate by the adsorbent determines the adsorption equilibrium time and can reflect the combining capacity and the removal efficiency, which can provide a basis for the design of the dynamic continuous flow system and its optimization design. The adsorption kinetics of fluoride by the SA-CMAC at different temperatures are presented in Fig. 6. The pseudo-first-order kinetics [33,34], pseudo-second order kinetics [35] and the intraparticle diffusion model [36,37] were adopted to analyze the experimental data and the linear equations were as follows:

$$\lg(Q_e-Q_t)=\lg Q_e-k_1 t \tag{6}$$

$$\frac{t}{Q_t}=\frac{1}{h}+\frac{t}{Q_e} \tag{7-1}$$

$$h=k_2 Q_e^2 \tag{7-2}$$

$$Q_t=k_{ip}t^{0.5}+C \tag{8}$$

where Q_e (mg/g) and Q_t (mg/g) are the adsorption capacity at the equilibrium time and t (h), respectively, k_1 (h^{-1}), k_2 (g $mg^{-1}\cdot h^{-1}$) and

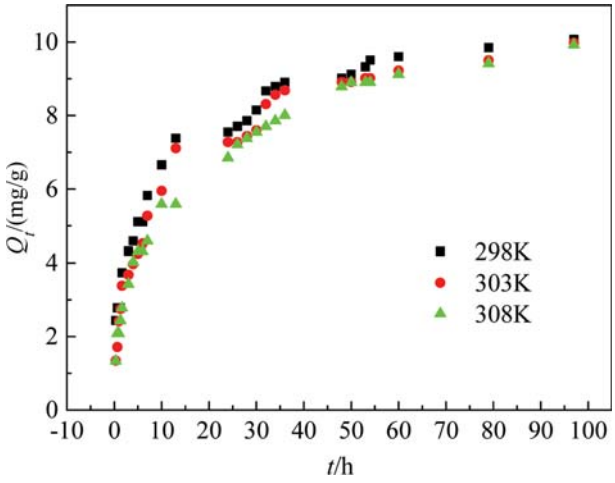

Fig. 6. Adsorption kinetics of fluoride by SA-CMAC.

Table 3. The adsorption isothermal parameters of fluoride by SA-CMAC

Kinetic equation	Temperature (K)		
	298	303	308
Pseudo-first-order			
Q_{exp} (mg g^{-1})	10.07	9.98	9.93
Q_{max} (mg g^{-1})	7.814	7.180	7.584
k_1 (h^{-1})	0.02290	0.01670	0.01570
R^2	0.9096	0.9591	0.9810
Pseudo-second order			
Q_{max} (mg g^{-1})	10.24	10.11	10.09
k_2 (mg g^{-1} $h^{-0.5}$)	0.01983	0.01641	0.01404
h (mg g^{-1} h^{-1})	0.003356	0.003300	0.003247
R^2	0.9940	0.9924	0.9893
Intraparticle diffusion			
k_{ip} (mg g^{-1} $h^{-0.5}$)	0.8997	0.9553	0.9640
C	2.817	2.126	1.819
R^2	0.9247	0.9263	0.9593

k_{ip} (mg g^{-1} $h^{-0.5}$) are the reaction rate constants of the pseudo-first-order kinetics, pseudo-second order kinetics and the intra-particle diffusion model, respectively, and h is the initial adsorption speed constant. The fitting results are presented in Table 3.

According to Table 3, the fitting coefficients (R^2) of the pseudo-second-order kinetics at different temperatures were higher than those of the pseudo-first-order kinetics, and the calculated theoretical values of Q_{max} were also more approximate to the experimental values. The results showe that the adsorption process of fluoride by the SA-CMAC complied with the pseudo-second-order reaction mechanism and the chemical adsorption was the limiting step of the adsorption reaction. Therefore, the removal process of fluoride by the SA-CMAC was controlled by the chemical reaction. The initial adsorption speed decreased with the increase of temperature, which showed that the elevated temperature went against the adsorption of fluoride by the SA-CMAC. Although the adsorption capacity of the triple-metal oxide might be reduced by calcium alginate hybridization and the equilibrium time might be prolonged, the millimeter-sized SA-CMAC was easy to separate, which is beneficial for the subsequent treatment process in practical applications.

5. Effect of Co-existing Ions on the Adsorption

Coexistent PO_4^{3-}, CO_3^{2-}, SO_4^{2-} and NO_3^- in the industrial wastewater [38] could affect the removal of F^- by the SA-CMAC. The effects of different concentrations of PO_4^{3-}, CO_3^{2-}, SO_4^{2-} and NO_3^- on the adsorption of fluoride by the SA-CMAC were investigated and the results are presented in Fig. 7. PO_4^{3-} and CO_3^{2-} had more significant effects on the adsorption process than the SO_4^{2-} and NO_3^-. The fluoride removal efficiency decreased greatly with the increase of the concentration of PO_4^{3-} and CO_3^{2-}. When the concentration increased to 0.1 mol /L, the adsorption rates of fluoride were only 0.38 mg g^{-1} and 3.66 mg/g, respectively. Accordingly, the adsorption removal efficiency decreased to 4.7% and 45.49%. The decrease of adsorption removal efficiency mainly could be attributed to the competition of the adsorptive sites by PO_4^{3-} and CO_3^{2-}.

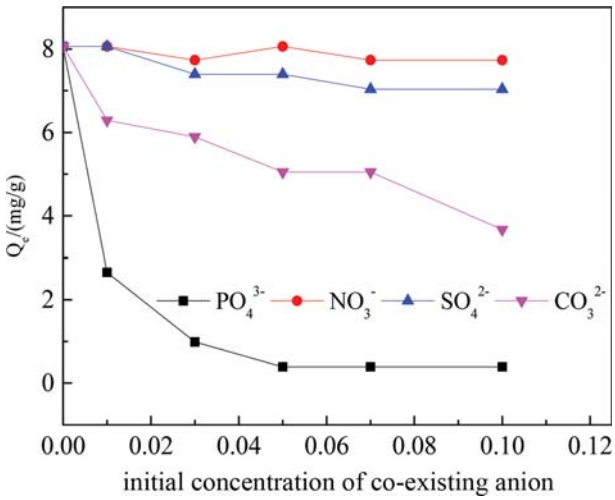

Fig. 7. Effect of co-existing anions on the adsorption of fluoride by the SA-CMAC.

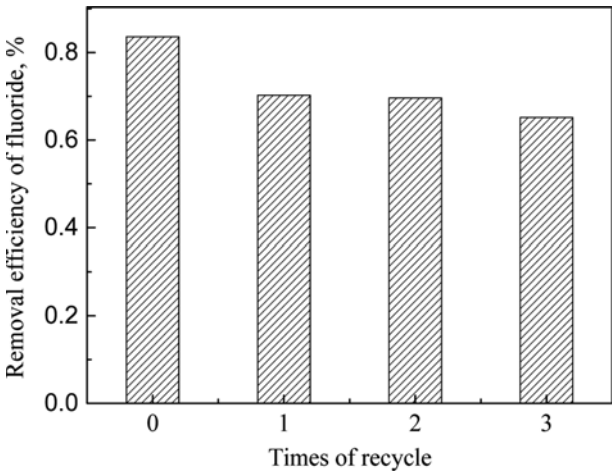

Fig. 8. Recycle study of the SA-CMAZ.

6. Regeneration of the Adsorbents

A concentrated solution containing fluoride can be obtained by the desorption process, which contributed to the recovery of fluoride and reuse of the adsorbents. Sodium hydroxide with a concentration of 0.01 mol L^{-1} was used as the desorption agent, and the result is presented in Fig. 8. The adsorption capacity decreased slightly with the recycle times. In the third cycle, the reclaimed adsorbents still could adsorb 65% of the total fluoride in the solution. The recycling of the SA-CMAC could reduce the operation costs and remove the fluoride in wastewater.

CONCLUSION

The adsorption performance of fluoride by the SA-CMAC was studied. Based on the results obtained, the following conclusions can be drawn:

(1) The prepared SA-CMAC particles had a better pH adaptation.

(2) The adsorption kinetics study showed that the adsorption

process fitted the pseudo-second-order kinetics model; the adsorption isotherms had a better adaptation to both Langmuir and Freundlich models. The calculated thermodynamic parameters suggested that the adsorption was a spontaneous, exothermic and entropy-reductive process.

(3) The effect order of the coexisting ions on the adsorption removal of fluoride was as follows: $PO_4^{3-}>CO_3^{2-}>SO_4^{2-}>NO_3^-$.

(4) SA-CMAC had a good recycling performance, and after three rounds of adsorption-desorption cycle, the SA-CMAC could still adsorb 65% of the fluoride in wastewater.

ACKNOWLEDGEMENTS

The authors gratefully acknowledge the Science Program of the Department of Education Hunan Province (2015C0260), Natural Science Foundation of Hunan Province China (2017JJ2020), Outstanding Youth Project of Hunan Province China (16B049), Key project of National Water Pollution Control and Management of Science and Technology of China (2010ZX07212008), Science and Technology project of Yiyang, Hunan Province (2015JZ26).

REFERENCES

1. L. Lv, J. He, M. Wei, D. Evans and X. Duan, *J. Hazard. Mater.*, **133**, 119 (2006).
2. X. Fan, *Water Res.*, **37**, 4929 (2003).
3. C. Liu and J. C. Liu, *J. Taiwan Inst. Chem. E.*, **58**, 259 (2016).
4. C. Y. Hu, S. L. Lo and W. H. Kuan, *J. Colloid Interface Sci.*, **283**, 472 (2005).
5. F. Shen, X. Chen, P. Gao and G. Chen, *Chem. Eng. Sci.*, **58**, 987 (2003).
6. K. Jiang, K. Zhou, Y. Yang and H. Du, *J. Environ. Sci.-China*, **25**, 1331 (2013).
7. L. Deng, Y. Liu, T. Huang and T. Sun, *Chem. Eng. J.*, **287**, 83 (2016).
8. A. Ezzeddine, N. Meftah and A. Hannachi, *Desalination Water Treatment*, **55**, 2618 (2015).
9. J. He, X. Cai, K. Chen, Y. Li, K. Zhang, Z. Jin, F. Meng, N. Liu, X. Wang, L. Kong, X. Huang and J. Liu, *J. Colloid Interface Sci.*, **484**, 162 (2016).
10. A. Bhatnagar, E. Kumar and M. Sillanpää, *Chem. Eng. J.*, **171**, 811 (2011).
11. S. Dong and Y. Wang, *Water Res.*, **88**, 852 (2016).
12. A. Dhillon, M. Nair, S. K. Bhargava and D. Kumar, *J. Colloid Interface Sci.*, **457**, 289 (2015).
13. P. Koilraj and S. Kannan, *Chem. Eng. J.*, **234**, 406 (2013).
14. D. Tang and G. Zhang, *Chem. Eng. J.*, **283**, 721 (2016).
15. H. Jiang, W. Zhang, P. Chen, Q. He, M. Li, L. Tian, Z. Tu and Y. Xu, *J. Inorg Organomet P.*, **26**, 285 (2016).
16. X. Dou, D. Mohan, C. U. Pittman Jr. and S. Yang, *Chem. Eng. J.*, **198-199**, 236 (2012).
17. T. Zhang, Q. Li, Y. Liu, Y. Duan and W. Zhang, *Chem. Eng. J.*, **168**, 665 (2011).
18. X. Zhao, L. Zhang, P. Xiong, W. Ma, N. Qian and W. Lu, *Micropor. Mesopor. Mater.*, **201**, 91 (2015).
19. D. Thakre, S. Jagtap, N. Sakhare, N. Labhsetwar, S. Meshram and S. Rayalu, *Chem. Eng. J.*, **158**, 315 (2010).
20. S. K. Swain, T. Patnaik, P. C. Patnaik, U. Jha and R. K. Dey, *Chem. Eng. J.*, **215-216**, 763 (2013).
21. Y. Chi, Y. Chen, C. Hu, Y. Wang and C. Liu, *J. Mol. Liq.*, **242**, 416 (2017).
22. L. Wu, X. Lin, X. Du and X. Luo, *J. Radioanal. Nucl. Ch.*, **310**, 1 (2016).
23. D. W. Cho, H. Song, B. Kim, F. W. Schwartz and B. H. Jeon, *Water, Air, Soil Pollution*, **226**, 1 (2015).
24. Y. Huo, W. Ding, X. Huang, J. Xu and M. Zhao, *Chinese J. Chem. Eng.*, **19**, 365 (2011).
25. J. Wang, D. Kang, X. Yu, M. Ge and Y. Chen, *Chem. Eng. J.*, **264**, 506 (2015).
26. W. Chen, Z. Y. Ouyang, C. Qian and H. Q. Yu, *Environ. Pollut.*, **233**, 1 (2017).
27. T. Lv, W. Ma, G. Xin, R. Wang, J. Xu, D. Liu, F. Liu and D. Pan, *J. Hazard. Mater.*, **237-238**, 121 (2012).
28. S. Liu, H. Wang, L. Chai and M. Li, *J. Colloid Interface Sci.*, **478**, 288 (2016).
29. Q. Chen, K. Zhou, Y. Chen, A. Wang and F. Liu, *Environ. Technol.*, **38**, 2824 (2017).
30. W. Yang, Q. Tang, J. Wei, Y. Ran, L. Chai and H. Wang, *Appl. Surf. Sci.*, **369**, 215 (2016).
31. Q. L. Zhang, N. Y. Gao, Y. C. Lin, B. Xu and L. S. Le, *Water Environ. Res.*, **79**, 931 (2007).
32. K. Zhang, S. Wu, J. He, L. Chen, X. Cai, K. Chen, Y. Li, B. Sun, D. Lin, G. Liu, L. Kong and J. Liu, *J. Colloid Interface Sci.*, **475**, 17 (2016).
33. W. Yang, Q. Tang, J. Wei, Y. Ran, L. Chai and H. Wang, *Appl. Surf. Sci.*, **369**, 215 (2016).
34. Q. Chen, K. Zhou, Y. Hu, F. Liu and A. Wang, *Water Sci. Technol.*, **75**, 1294 (2017).
35. C. Peng, L. Chai, C. Tang, X. Min, Y. Song, C. Duan and C. Yu, *J. Environ. Sci.-China*, **51**, 222 (2017).
36. W. Ma, F. Ya, M. Han and R. Wang, *J. Hazard. Mater.*, **143**, 296 (2007).
37. R. Chen, L. Chai, Q. Li, Y. Shi, Y. Wang and A. Mohammad, *Environ. Sci. Pollut. Res. Int.*, **20**, 7175 (2013).
38. J. Cai, Y. Zhang, B. Pan, W. Zhang, L. Lv and Q. Zhang, *Water Res.*, **102**, 109 (2016).